

Helical Discotic Liquid Crystals

Libor Vyklický,[†] S. Holger Eichhorn,^{*,‡} and Thomas J. Katz^{*,†}

Department of Chemistry, Columbia University, New York, New York, 10027, and
Department of Chemistry and Biochemistry, University of Windsor, Windsor,
Ontario, Canada N9B 3P4

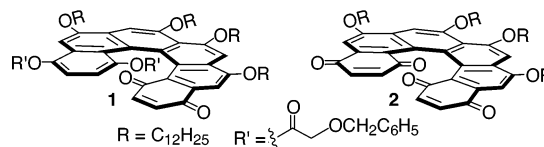
Received March 12, 2003. Revised Manuscript Received June 24, 2003

The structural properties of ten helicenebisquinones that have side chains differing in number and structure are analyzed by means of polarized light microscopy, differential thermal analysis, and X-ray diffraction. All the derivatives whose side chains are bonded to the helical cores by ether linkages assemble into hexagonally arrayed columns, even when the number of side chains is only two, but not all form true liquid crystalline phases. Those that have three unsymmetrically disposed side chains do, and when these side chains are dodecyloxymethoxy groups, the clearing temperatures are as low as 107 °C, which is 125 °C lower than that of the only previously studied nonracemic helicenebisquinone. Differences in side chain chirality affect the melting characteristics moderately, but they affect the packing arrangements, as analyzed by X-ray diffraction, insignificantly. A set of models is proposed to account for the differences in the materials' properties.

Introduction

It is remarkable how much less is known about nonracemic chiral liquid crystals that are discotic than about those that are calamitic, and especially when the chirality is in the core of the molecules rather than in the side chains.¹ In fact there is only one example that has a twisted aromatic core.² Its molecular structure, **1**, is related to that of helicene **2**.³ Molecules of both **1** and **2** stack into columns when the materials are pure^{1,3} or dissolved in saturated hydrocarbon solvents.^{1,3,4} The enantiopure columnar structures exhibit significant optical properties, including some unprecedented. The specific rotatory power of **2**'s aggregates is enormous,^{3a,c,d} and interleaved layers of its enantiomers generate intense quasi-phase matched second harmonics.⁵ Electric fields reorient the columns of **1** in dodecane,⁴ and,

as shown for a related structure, reverse the signs of the second harmonics' circular difference effects.^{5e}



In the pure materials, the columns pack into hexagonal arrays.^{1,3b} In **2** these arrays crystallize into long fibers that are easily seen under an optical microscope and that melt into an isotropic fluid at ca. 210 °C.^{3d,6} At this high temperature the molecules also racemize at an appreciable rate,^{3a} which is unfortunate, because racemic **2** gives rise to neither the long columnar assemblies nor the intense second harmonics of the enantiomerically pure material.^{3a,5b} But **1** melts at much lower temperature. It is liquid crystalline at room temperature and becomes isotropic at 85 °C.¹

In this paper we show that derivatives of **2** also can have thermotropic liquid crystalline phases. The numbers and types of side chains just have to be modified. We show how some of the modifications affect the mesomorphic properties. The structures studied had cores **3–5** and side chains OC₁₂H₂₅, OCH₂OC₁₂H₂₅, OCO(CH₂)₂SC₁₂H₂₅, and **6–8**. Table 1 shows how these cores and side chains were combined, and it provides the symbolism used to identify the different compounds.

Results

Syntheses. The [6]helicenebisquinones with two and four side chains, +**H2C12** and +**H4C12**, were prepared and characterized previously.^{3d,7} Those with three side chains were prepared by procedures analogous to those

* Authors to whom correspondence should be addressed. T.J.K. E-mail: tjkl@columbia.edu. S.H.E. E-mail: eichhorn@uwindsor.ca.

[†] Columbia University.

[‡] University of Windsor.

(1) Nuckolls, C.; Katz, T. J. *J. Am. Chem. Soc.* **1998**, *120*, 9541.

(2) There are a few chiral discotics whose cores are saccharides, inositols, or cyclotrimeratrylene. Footnotes 2–4 in ref 1 refers to them. There are some that have helically twisted aromatic cores, but they are racemic. Footnote 5 in ref 1 refers to them.

(3) (a) Nuckolls, C.; Katz, T. J.; Katz, G.; Collings, P. J.; Castellanos, L. *J. Am. Chem. Soc.* **1999**, *121*, 79. (b) Lovinger, A. J.; Nuckolls, C.; Katz, T. J. *J. Am. Chem. Soc.* **1998**, *120*, 264. (c) Nuckolls, C.; Katz, T. J.; Verbiest, T.; Van Elshocht, S.; Kauranen, M.; Kuball, H.-G.; Kiesewalter, S.; Lovinger, A. J.; Persoons, A. *J. Am. Chem. Soc.* **1998**, *120*, 8656. (d) Nuckolls, C.; Katz, T. J.; Castellanos, L. *J. Am. Chem. Soc.* **1996**, *118*, 3767.

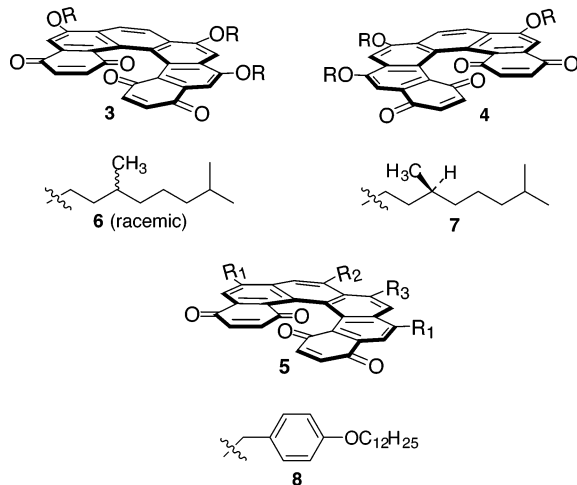
(4) Nuckolls, C.; Shao, R.; Jang, W.-G.; Clark, N. A.; Walba, D. M.; Katz, T. J. *Chem. Mater.* **2002**, *14*, 773.

(5) (a) Busson, B.; Kauranen, M.; Nuckolls, C.; Katz, T. J.; Persoons, A. *Phys. Rev. Lett.* **2000**, *84*, 79. (b) Verbiest, T.; Van Elshocht, S.; Kauranen, M.; Hellemans, L.; Snaauwaert, J.; Nuckolls, C.; Katz, T. J.; Persoons, A. *Science* **1998**, *282*, 913. (c) Van Elshocht, S.; Verbiest, T.; de Schaetzen, G.; Hellemans, L.; Phillips, K. E. S.; Nuckolls, C.; Katz, T. J.; Persoons, A. *Chem. Phys. Lett.* **2000**, *323*, 340. (d) Verbiest, T.; Van Elshocht, S.; Persoons, A.; Nuckolls, C.; Phillips, K. E. S.; Katz, T. J. *Langmuir* **2001**, *17*, 4685. (e) Verbiest, T.; Sioncke, S.; Persoons, A.; Vyklický, L.; Katz, T. J. *Angew. Chem., Int. Ed.* **2002**, *41*, 3882.

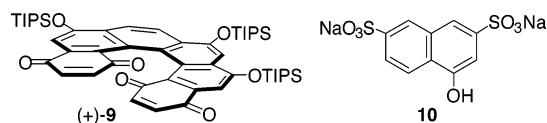
(6) The transition temperature measured here by DSC (see Table 2) is 236 °C.

Table 1. Compounds Studied and Symbols Used to Identify Them

core	side chain	symbol
3	6	+H3C10rac
3	7	+H3C10S
4	7	-H3C10S
3	8	+H3bn12
5	R ₁ = OC ₁₂ H ₂₅ , R ₂ = R ₃ = H	+H2C12
5	R ₁ = R ₃ = OC ₁₂ H ₂₅ , R ₂ = H	+H3C12
5	R ₁ = R ₂ = R ₃ = OC ₁₂ H ₂₅	+H4C12
3	R = CH ₂ OC ₁₂ H ₂₅	+H3C130
3	R = COC ₂ H ₄ SC ₁₂ H ₂₅	+H3C14S
3 + 4 (racemic)	R = COC ₂ H ₄ SC ₁₂ H ₂₅	±H3C14S



used before.⁸ Thus racemic and enantiomerically pure tris(triisopropylsiloxy)[6]helicenebisquinones (\pm)-**9**, (+)-**9**, and (–)-**9**, synthesized from disodium 4-hydroxy-naphthalene-2,7-disulfonate (**10**),⁸ were combined either with 3,7-dimethyl-1-iodooctane^{9,10} and Bu₄NF in THF or with 1-iodomethyl-4-dodecyloxy-benzene,^{11,12} chloromethoxydodecane,¹³ or 3-(dodecylthio)propanoyl chloride¹⁴ and CsF in DMF.



The spectroscopic and other analyses, specified in the Experimental Section, were appropriate for the structures assigned. The absolute configurations of (+)- and (–)-**9** were assigned previously.⁸

(7) Katz, T. J.; Liu, L.; Willmore, N. D.; Fox, J. M.; Rheingold, A. L.; Shi, S.; Nuckolls, C. P.; Rickman, B. H. *J. Am. Chem. Soc.* **1997**, *119*, 10054.

(8) Paruch, K.; Vyklický, L.; Katz, T. J.; Incarvito, C. D.; Rheingold, A. L. *J. Org. Chem.* **2000**, *65*, 8774.

(9) Unlike Bu₄NF in THF, CsF, the reagent used in ref 8, gave only inseparable mixtures and none of the desired product. Bu₄NF in THF also gave more reproducible results than CsF when applied to the preparations of **H3C12** and some other alkoxy[6]helicenebisquinones.

(10) For previous syntheses, see: (a) Chen, C. Y.; Nagai, S.; Akita, H. *Chem. Pharm. Bull.* **1996**, *44*, 2153. (b) Nagai, K. *Bull. Chem. Soc. Jpn.* **1976**, *49*, 265. The chemical shifts of the CH₃ and CH₂ ¹H NMRs are those in the latter reference.

(11) (a) Fox, J. M.; Goldberg, N. R.; Katz, T. J. *J. Org. Chem.* **1998**, *63*, 7456. (b) Paruch, K.; Katz, T. J.; Incarvito, C.; Lam, K.-C.; Rhatigan, B.; Rheingold, A. L. *J. Org. Chem.* **2000**, *65*, 7602.

(12) The step was modeled on a procedure in Bandgar, B. P.; Sadavarte, V. S.; Uppalla, L. S. *Tetrahedron Lett.* **2001**, *42*, 951.

(13) Shipov, A. G.; Savostyanova, I. A.; Baukov, Y. I. *J. Gen. Chem. USSR* **1989**, 1067.

(14) Rapoport, L.; Smith, A.; Newman, M. S. *J. Am. Chem. Soc.* **1947**, *69*, 693.

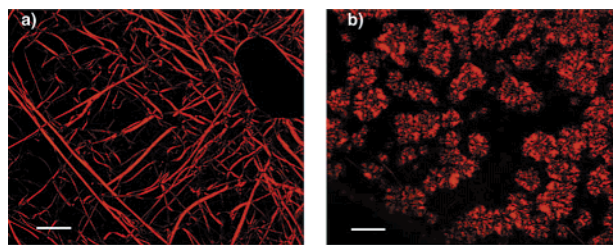


Figure 1. Polarized light microscopic images of (a) **+H3C12** at 220 °C and (b) **+H2C12** at 204 °C. The samples had been heated to the clearing temperatures (230 °C and 220 °C, respectively) and then cooled. The white bars are 0.1 mm long.

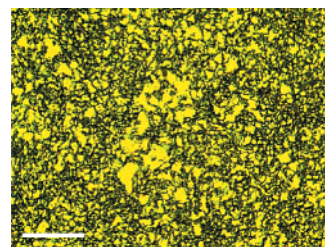


Figure 2. Photomicrograph (200× magnification) showing the grainy texture of \pm **H3C14S** at 100 °C between crossed polarizers. The white bar is 0.1 mm long.

Polarized Light Microscopy. Polarized light microscopy shows that, when heated, each of the materials except **+H3C14S**, which is an isotropic wax at room temperature, undergoes a transformation from a phase that is anisotropic to one that is isotropic. Between 50 and 100 °C the samples all soften, indicative of a transition from an anisotropic glassy solid phase to an anisotropic mesophase. But, except for glass transitions at 40 °C exhibited by \pm **H3C14S** and at 68 °C by **+H3C10S**, the only changes detectable by differential scanning calorimetry are transitions to isotropic states (see below). **+H3C130** and **+H3bn12** are sticky even at 25 °C. When **+H3C12** and **+2HC12** are cooled from their isotropic melts, they give rise to distinctly different textures. Like those of **2**,^{3d} the anisotropic phases of **+H3C12** self-organize into fibrous structures, displayed in Figure 1a, whereas the anisotropic phases of **+H2C12** emerge from the isotropic melt as crystalline-appearing spherulites (Figure 1b). All the other anisotropic phases exhibit grainy textures of small domains that are of little analytical value. The natural texture of \pm **H3C14S** at 100 °C (that is, the texture observed when the isotropic liquid is cooled) is shown in Figure 2. The textures are not changed significantly if the glass surfaces are modified by rubbing, by coating with polyimide and subsequently rubbing, or by coating with octadecyl-trichlorosilane. However, mechanically shearing those samples that are most fluid—that is those with clearing temperatures below 180 °C—homogeneously aligns them. Figure 3 illustrates this for a sample of **+H3C130** at 50 °C.

Differential Scanning Calorimetry. Table 2 summarizes the results of differential scanning calorimetric measurements. At high temperatures all the materials display reversible transitions from mesophases to isotropic liquids, with enthalpy changes between 10 and 40 kJ/mol. The only transitions between solid states and mesophases, both broad glass transitions unaccompanied by texture changes, are those of \pm **H3C14S** (at 40 °C) and **+H3C10S** (at 68 °C). Softening, which for

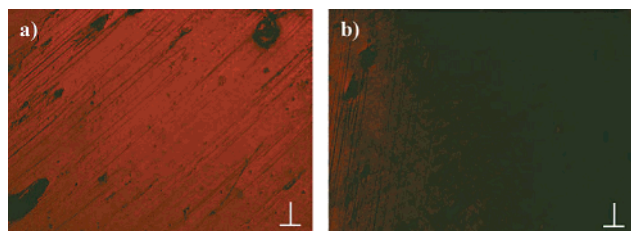


Figure 3. Polarized light photomicrographs at 100 \times magnification of a film of +H3C13O at 50 $^{\circ}$ C that had been aligned by shearing (a) at 45 $^{\circ}$ to the direction (marked at the lower right) of the crossed polarizers and (b) parallel to one of the crossed polarizers.

Table 2. Mesophase to Isotropic Transition Temperatures ($^{\circ}$ C) and Enthalpies (kJ mol^{-1}) Measured by DSC during the Second Heating^a (T , Heating) and First Cooling (T , Cooling) Cycles (the Temperatures Were Scanned at 10 $^{\circ}$ C/min)

compound	T , heating	T , cooling
+H3C10S	68 ^f , 173.1 (18.69) ^b	65 ^f , 171.2 (−15.78)
−H3C10S	149.6 (9.80)	146.4 (−8.99)
+H3C10rac	161.2 (12.81) ^b	159.7 (−12.42)
+H2C12	208.5 (54.70) ^c	161.1 (−0.78) ^d
		185.9 (−15.75) ^d
+H3C12	219.8 (56.36) ^c	180.1 (−2.58) ^d
		206.3 (−11.49) ^d
+H4C12	236 (ca. 45) ^{c,e}	195.6 (−3.66) ^d
		219.8 (−24.71) ^d
±H3C14S	40 ^f	40 ^f
	125.3 (39.79)	84.2 (−27.43)
+H3bn12	190.4 (16.39) ^b	185.2 (−13.55)
+H3C13O	107.2 (17.49)	104.2 (−18.61)

^a Except as noted. ^b On the first cycle the peak was sharp and the enthalpy ca. 6 kJ/mol higher. On subsequent cycles, the peak was broad. ^c First heating cycle. ^d Because the sample partially racemized during the first heating cycle, two transitions were seen in the second cycle. ^e Racemization and decomposition start at ca. 230 $^{\circ}$ C. ^f Glass transition.

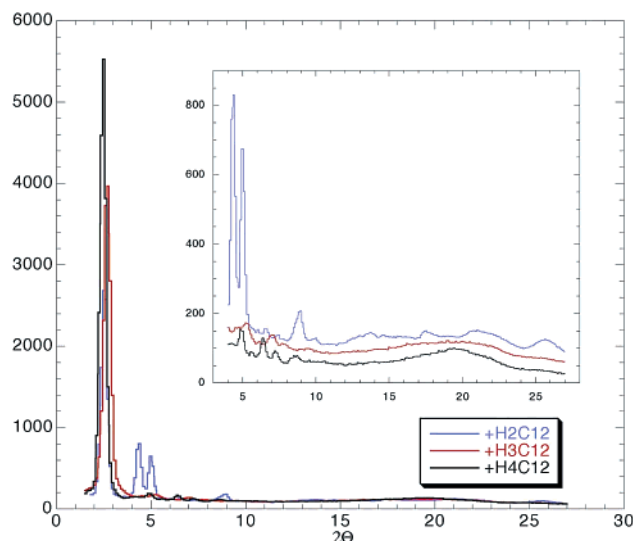


Figure 4. X-ray diffraction patterns from +H2C12, +H3C12, and +H4C12 at 120 $^{\circ}$ C. The insert shows magnified views of the diffractions at wide angles.

all the other compounds was observable by optical microscopy and X-ray diffraction, was not signaled by the DSCs.

X-ray Diffraction Analyses. Figures 4–6 show the diffraction patterns from a number of samples: Figure 4 shows those from +H2C12, +H3C12, and +H4C12 at 120 $^{\circ}$ C; Figure 5 shows those from +H3C10rac,

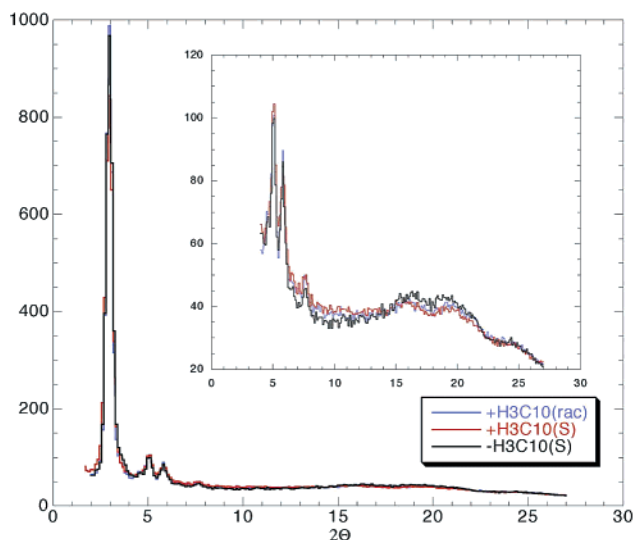


Figure 5. X-ray diffraction patterns from +H3C10rac, +H3C10S, and −H3C10S at 120 $^{\circ}$ C. The insert shows magnified views of the diffractions at wide angles.

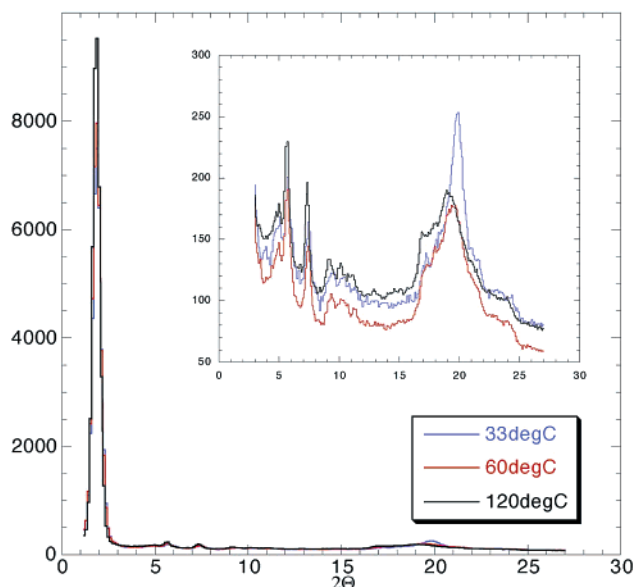


Figure 6. X-ray diffraction patterns from ±H3C14S at three temperatures. The insert shows magnified views of the diffractions at wide angles.

+H3C10S, and −H3C10S at 120 $^{\circ}$ C; and Figure 6 shows those from ±H3C14S at three temperatures. Table 3 summarizes all the X-ray diffraction measurements. The analyses show that when the temperatures are raised from 30 to 120 $^{\circ}$ C or higher, the phases of all the samples except that of ±H3C14S change from being partially crystalline and somewhat ordered in hexagonal columns to being well-ordered in hexagonal columnar mesophases. But these phases do not revert to the original states when the samples are recooled to 25 $^{\circ}$ C. The intercolumnar distances analyzed from these measurements, between 34 and 45 Å, are approximately those expected if the side chains are liquidlike¹⁵ or interdigitated. Unusual, however, was the observation that the intercolumnar spacings decrease or stay constant when the temperatures decrease, whereas in most

(15) Engel, M. K.; Bassoul, P.; Bosio, L.; Lehmann, H.; Hanack, M.; Simon, J. *Liq. Cryst.* **1993**, *15*, 709.

Table 3. Peaks in the X-ray Diffractions from the Helicene Samples at Various Temperatures (T) and their Assignments^a

compound	interlayer distances in Å (<i>hkl</i>)	iIntercolumnar spacing (Å)	T (°C)
+H3C10S ^b	29.6 (100), 17.2 (110), 14.9 (200), 11.4 (210)	34.5	30
	30.0 (100), 17.2 (110), 15.1 (200), 11.4 (210)	34.6	120
−H3C10S ^b	29.1 (100), 17.2 (110), 14.8 (200), 11.4 (210)	33.6	30
	29.7 (100), 17.4 (110), 15.1 (200), 11.4 (210)	34.3	120
+H3C10rac ^b	29.3 (100), 17.2 (110), 14.8 (200), 11.3 (210)	33.8	30
	29.7 (100), 17.4 (110), 15.1 (200), 11.5 (210)	34.3	120
+H2C12 ^c	33.7 (100), 27.4, 20.1 (110), 17.3 (200), 14.0, ^e 10.5 ^e		30
	34.6 (100), 20.5 (110), 17.6 (200), 13.4 (210), 10.1 (220), 5.1 ^e , 3.5 ^f	39.9	120
	34.6 (100), 20.5 (110), 17.6 (200), 13.4 (210), 10.1 (220), 5.1 ^e , 3.5 ^f	39.9	150
	34.6 (100), 20.5 (110), 17.6 (200), 13.4 (210), 10.1 (220), 5.1 ^e , 3.5 ^f		
		39.9	190
+H3C12	32.9 (100), 19.1 (110), 32.9 (100), 18.8 (110), 16.7 (200)	38.0	30
	32.9 (100), 19.0 (110), 16.5 (200)	38.0	120
		38.0	170
+H4C12	34.7 (100), 17.6 (200), 13.3 (210), 11.8 (300)	40.1	30
	35.2 (100), 20.8 (110), 17.7 (200), 13.8 (210), 12.3 (300), 10.3 (220)	40.6	120
	36.0 (100), 21.0 (110), 18.0 (200), 14.0 (210), 12.4 (300), 10.7 (220)	41.6	205
±H3C14S ^d	46.5, 23.2, 17.7, 15.6, 12.1	46.5	30
	46.5, 17.7, 15.6, 12.1	46.5	60
	46.5, 17.7, 15.6, 12.1	46.5	120
+H3bn12	38.9 (100), 21.8 (110), 14.5 (210), 3.9, ^e 3.6	44.9	30
	38.9 (100), 21.8 (110), 18.8 (200), 14.5 (210), 4.0, ^e 3.6 ^f	44.9	120
	39.9 (100), 25.1 (110), 19.6 (200), 13.2 (300), 4.0, ^e 3.6 ^f	46.1	185
+H3C13O	33.1 (100), 19.7 (110), 16.9 (200), 12.8 (210), 11.3 ^e	38.2	30
	33.1 (100), 19.7 (110), 16.9 (200), 12.8 (210), 11.3 ^e	38.2	100

^a All samples displayed a broad (halo) reflection at about 4.5 Å, typical of the amorphous side chains of columnar discotic liquid crystals.

^b The side chain halo was split into equally intense broad peaks at ca. 5.3 and ca. 4.6 Å as displayed in Figure 5. ^c Additional small peaks that gained intensity with increasing temperature were found at about 12.1 and 8.9 Å. ^d Unknown mesophase. The side chain reflection at 4.5 Å is relatively sharp and intense at 30 °C. It broadens when the sample is heated, but at 60 and 120 °C it remains sharper and more intense than the typical halos from the other helicenes. There are at least four less-intense but sharp peaks in the region between 9.8 and 6.8 Å. These do not change with temperature. ^e Diffraction peak of very low intensity that remains unassigned. ^f Tentatively assigned, by analogy with assignments of broad diffractions between 3.4 and 3.6 Å from discotic columnar mesophases, to close and periodic π - π stacking of helicene cores.

discotic liquid crystals, the spacings increase. This increase has been attributed to the side chains stiffening into their most extended all-trans conformations.¹⁵ The decreases upon cooling found here might be explained by side chain interdigitation increasing at low temperatures. The few side chains attached to the helicene cores can fill the space between the columnar stacks only if they are in a nonextended, molten state. When cooling stiffens them, the resulting voids may be filled by the side chains of neighboring columns. Thus, the expanded spacing that should result from an increased extension of the side chains is more than compensated by increased interdigitation.

The X-ray diffractions from compounds +H2C12, +H3C12, and +H4C12 at 120 °C show only peaks characteristic of hexagonal columnar mesophases, but in one case there are additional peaks at wide-angles. The magnified views in Figure 4 show that the diffraction from +H2C12, unlike that from the other compounds, includes many peaks in the wide-angle region, indicative of a high degree of crystallinity. (The other compounds show at wide-angles only the typical halos at ca. 4.5 Å, characteristic of the diffraction from the side chains of liquid crystals.) Also, for +H2C12, the (110), (220), and (200) diffraction peaks are much stronger than those for the other compounds. The implication is that molecules of +H2C12 are the most organized. But it is surprising, if this is so, that +H2C12 has the lowest melting point of the three substances.

Interesting about the diffraction patterns in Figure 5, of the compounds with 3,7-dimethyloctyloxy side chains (+H3C10rac, +H3C10S, and −H3C10S), is that

in all three cases the side chain halos are split into two peaks of equal intensity. Those at ca. 4.6 Å can be assigned to the aliphatic chains on adjacent stacked molecules, but the peaks at 5.3 Å can be attributed to intracolumnar packing and suggest that the helicene cores stack loosely. Figure 7 indicates this by showing that helicenes that freely rotate about the axes of columns in which they are stacked (Figure 7A and B) should be separated by 5 to 6 Å, whereas those that are packed tightly (Figure 7C) should be separated by the π - π -stacking distance in discotic liquid crystals, ca. 3.6 Å.

±H3C14S is the one compound that does not organize into a hexagonal columnar mesophase. However, we cannot tell which phase it does assume. All we note is that the diffraction pattern is complex and a glass transition at 40 °C, observed by polarizing microscopy and DSC, broadens the side chain halo at ca. 4.5 Å (Figure 6) and, as for the other mesophases studied here, improves the packing irreversibly.

Discussion

Their helical cores, wedge-shaped forms, lateral dipole moments, small number of side chains, and unsymmetrical disposition of those side chains differentiate the helicene derivatives studied here from most other discotics. We suggest that there are three ways, shown in Figure 7, that the helicene cores might organize into columnar stacks. (a) They might rotate more-or-less freely, giving rise to a truly liquid crystalline hexagonal columnar mesophase. (b) Because their lateral dipoles and wedge shapes might favor it, they might pack into

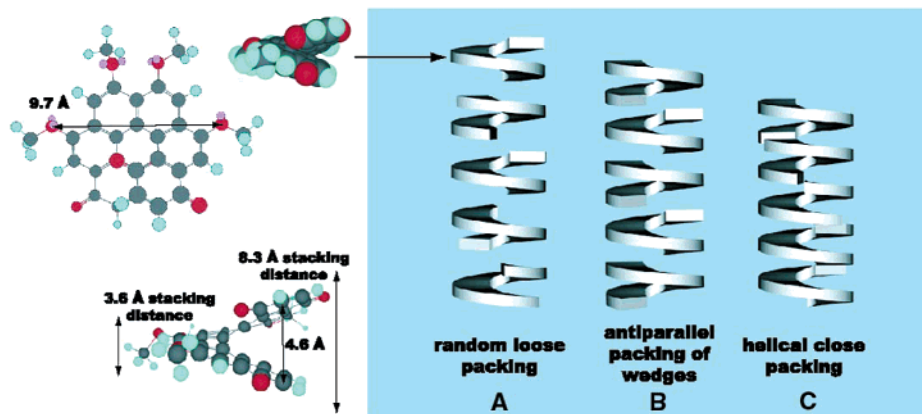


Figure 7. Dimensions of the helicene molecules and models showing how they might pack into columns.

an antiparallel arrangement^{16c} which is more ordered and can be described as a plastic crystalline phase if the positional order is three-dimensional or a liquid crystalline phase if it is two-dimensional. (c) Because of π - π interactions, they might pack closely into helices with 3–4 molecules per turn, with the high degree of order giving rise to a crystalline or plastic crystalline phase.^{16,17}

+**H2C12**, +**H3C12**, and +**H4C12** differ only in the number of dodecyloxy side chains attached to their cores. The clearing temperatures and transition enthalpies of all three are much higher than those of the compounds that have branched, rather than straight, side chains. This is not surprising.¹⁸ What is surprising is that as the number of side chains decrease, so do the clearing temperatures.¹⁹ Thus, according to DSC analyses, the material with four side chains (+**H4C12**) clears at ca. 236 °C, that with three side chains (+**H3C12**) clears at 220 °C, and that with two side chains (+**H2C12**) clears at 209 °C. This is significant because the samples racemize appreciably between ca. 220 and 230 °C^{3a,7} and decompose, according to thermogravimetric-differential thermal analyses, above 230 °C. Accordingly, of the three, only +**H2C12** and +**H3C12** can be melted reversibly into the isotropic state, and only +**H2C12** can be kept in its isotropic state for appreciable time without racemizing.

The absence of sharp X-ray diffraction peaks from their side chains implies that between room temperature and the temperature of their isotropic transitions

the molecules of all three of these materials pack in noncrystalline hexagonally arrayed columns. Slight (and irreversible) changes in the diffraction patterns when the temperatures are increased to 120 or 205 °C can be attributed to packing improving when viscosity decreases.

As expected, the core–core interaction is the greatest in +**H2C12**, the derivative that has only two side chains. The high intensity of the higher order peaks from the hexagonal lattice (Figure 4) indicates that the long-range correlation between the columns is substantial, and the reflection at 3.5 Å suggests that the intracolumnar packing of the helicene cores is tight, in accord with the helical columnar superstructure illustrated in model C of Figure 7. The broad peak at 4.5 Å implies that the side chains are noncrystalline and therefore that the material is in a mesophase. It might, therefore, be a plastic crystalline columnar phase.^{16b} A helical columnar twist also accounts for why an aromatic core with only two side chains—usually insufficient²⁰—gives a hexagonal columnar mesophase. The helical twist allows the two side chains to fill the column's space.

Of the three compounds, +**H3C12** is the only one that behaves like a typical liquid crystal. It alone shows the simple X-ray diffraction pattern characteristic of hexagonal columnar mesophases, with no additional peaks. In contrast, +**H4C12**, like +**H2C12**, shows additional peaks at ca. 12.3 and 10.5 Å. (However, unlike +**H2C12**, +**H4C12** exhibits no additional peaks at ca. 3.5 and 5.5 Å.) The less symmetrical substitution pattern of +**H3C12** presumably increases the disorder of the side chains and therefore promotes liquid crystallinity.²¹ The increased disorder would also account for the intercolumnar spacing being lower in +**H3C12** than in +**H2C12**. +**H3C12** and +**H4C12** might best be described by the packing models A or B in Figure 7.

Because it was the structure with three side chains that behaved like a discotic liquid crystal, it was molecules with three side chains that were subsequently studied to see how varying side chains affect the properties of related materials. One set of molecules was

(16) (a) Werth, M.; Vallerien, S. U.; Spiess, H. W. *Liq. Cryst.* **1991**, *10*, 759. (b) Glösen, B.; Heitz, W.; Kettner, A.; Wendorff, J. H. *Liq. Cryst.* **1996**, *20*, 627. (c) Glösen, B.; Kettner, A.; Wendorff, J. H. *Mol. Cryst. Liq. Cryst.* **1997**, *303*, 115.

(17) Simmerer, J.; Glösen, B.; Paulus, W.; Kettner, A.; Schuhmacher, P.; Adam, D.; Etzbach, K.-H.; Siemensmeyer, K.; Wendorff, J. H.; Ringsdorf, H.; Haarer, D. *Adv. Mater.* **1996**, *8*, 815.

(18) The clearing temperatures of octa-(3,7-dimethyloctyloxy)phthalocyanines, both when the side chains are enantiopure and when they are racemic, are at least 50 °C lower than the clearing temperature of an octaoctyloxyphthalocyanine. (a) van Nostrum, C. F.; Bosman, A. W.; Gelinck, G. H.; Schouten, P. G.; Warman, J. M.; Kentgens, A. P. M.; Devillers, M. A. C.; Meijerink, A.; Picken, S. J.; Sohling, U.; Schouten, A.-J.; Nolte, R. J. M. *Chem. Eur. J.* **1995**, *1*, 171. (b) van der Pol, J. F.; Neeleman, E.; Zwicker, J. W.; Nolte, R. J. M.; Drenth, W.; Aerts, J.; Visser, R.; Picken, S. J. *Liq. Cryst.* **1989**, *6*, 577. Branching stabilizes other discotic mesophases by lowering the crystalline-to-mesophase transition temperature: Collard, D. M.; Lillya, C. P. *J. Am. Chem. Soc.* **1989**, *111*, 1829.

(19) The opposite is seen, for example, in copper complexes of 2-phenylazomethinopyridine (Lai, C. K.; Wang, K.-W.; Lin, R. *J. Mater. Chem.* **1998**, *8*, 2379) and in conventional discotic liquid crystals (Reference 20).

(20) Cammidge, A. N.; Bushby, R. J. In *Handbook of Liquid Crystals*; Demus, D.; Goodby, J., Gray, G. W., Spiess, H.-W., Vill, V., Eds.; Wiley-VCH: Weinheim, 1999; Vol 2B, p 693, and references therein.

(21) Eichhorn, H.; Wohrle, D.; Pressner, D. *Liq. Cryst.* **1997**, *22*, 643.

composed of diastereomers. In one pair (+**H3C10S** and -**H3C10S**) the centers of chirality in the side chains were identical, but the cores to which they were attached were opposite in chirality. In a related material (+**H3C10rac**), the side chains attached to the enantiopure core derived from racemic precursors, which means that the material was a complex mixture of diastereomers. The observation was, as Table 2 shows, that although +**H3C10S** and -**H3C10S** differ only in the chirality of their cores, the temperatures of their transitions from liquid crystalline to isotropic states differ by 24 °C and the enthalpies accompanying these transitions differ by 8 kJ/mol. The figures for the mixture of diastereomers +**H3C10rac** are between these two. The implication is that the chiral centers in the side chains significantly alter the core–core attractions. These are most perturbed in -**H3C10S** (and +**H3C10R**), least in +**H3C10S** (or -**H3C10R**), and intermediate in the derivative with the racemic side chains, +**H3C10rac**. Despite these differences in melting properties, no significant differences between the structures of the three materials' mesophases are detected when unaligned samples are analyzed by X-ray diffraction.²² All three stereoisomers display the same hexagonal columnar mesophases. None show peaks at ca. 3.5 Å, like those observed in the diffraction patterns from **1**¹ and from +**H2C12** (Table 3), ascribed in those cases to reflections from within ordered columnar stacks. However, all three display pairs of broad X-ray diffraction peaks of equal intensity at 5.3 and 4.6 Å. The peak at 4.6 Å is a halo characteristic of amorphous aliphatic side chains.^{1,23} The peak at 5.3 Å could arise from loosely packed helicene cores stacking as illustrated in packing model A in Figure 7, a plausible hypothesis as branched side chains are known to interfere with close core–core packing.²⁰

When oxygen atoms are incorporated into the side chains, in +**H3C13O**, the clearing temperature is drastically reduced, from 220 °C to 107 °C, a change whose direction accords with the scant literature on the affect of oxygen-substitution on melting points. In the case of triphenylene, benzene, and cyclotriveratrylene polyalkanoates, with the exception of 3-oxaalkanoates,^{24,25} the effect of oxygen substitution is to lower melting points^{25,26} and in the case of poly(ethylene oxide)s is to do essentially nothing.²⁷ The mesophase of +**H3C13O** is the most fluid of all those studied and, in consequence, the most easily aligned by shear. That it is fluid hexagonal columnar and probably describable by packing model A is implied by the paucity of reflections in its X-ray diffractogram and relatively small transition enthalpy. When in addition to oxygens, benzene rings are incorporated into the side chains, in *p*-dodecyloxybenzyloxy groups (in +**H3bn12**), the clearing temperature rises again, to 190 °C, and X-ray diffraction peaks

appear at 3.6 and 4.0 Å, showing that the regularity of intramolecular stacking has increased. The benzene rings appear to make the cores stack more tightly, just as they do in other discotic liquid crystals that have benzene-substituted side chains.²⁸ However, the enthalpy of its clearing transition remains as low as that of +**H3C13O**.

In ±**H3C14S** and +**H3C14S** the side chains are linked to the core by ester groups and the aliphatic chains contain thioether functions. The enantiopure material does not aggregate or form a liquid crystalline phase, whereas the racemic material does. Its X-ray diffraction pattern differs significantly from those of the other materials in Table 3. The 46 Å spacing, approximately the molecular diameter, suggests that the molecules are organized in layers rather than in hexagonally packed columns. The formation of a mesophase is indicated by a glass transition at 40 °C accompanied by a broadening of the side chain halo in the X-ray diffraction pattern. The relatively high enthalpy change at the clearing transition and the many sharp peaks observed in the small angle region of the diffraction pattern are indicative of high packing order. This mesophase is therefore likely to be a plastic crystal rather than a liquid crystal. The ester groups so drastically alter the properties that the packing probably differs from that of any of the models in Figure 7.^{16a,29}

Summary

Although the type and number of side chains attached to the helicene cores significantly alter how the molecules pack in their mesophases, in all cases but one the packing is hexagonal columnar. Even a derivative with only two chains, +**H2C12**, forms a hexagonal columnar mesophase. True liquid crystalline columnar mesophases form when there are three unsymmetrically disposed side chains. An example in which these side chains are dodecyloxymethoxy groups clears at 107 °C, very much lower than the temperature at which the only previously studied nonracemic [6]helicenebisquinone, which has four dodecyl side chains, clears. The materials with unbranched side chains are more viscous than the others and their mesophases appear to be plastic crystalline rather than liquid crystalline.

The packing models in Figure 7 explain, at least tentatively, the differences in the polarized light microscopic, thermal, and X-ray diffraction analyses. Although CD and X-ray diffraction analyses of single domains at different temperatures might elucidate the structures of the mesophases more definitively, the challenges associated with aligning the samples and carrying out such experiments at the required high temperatures have not yet been overcome.

Experimental Section

Physical Analyses. A Leica DMRXP polarizing microscope equipped with a Wild Leitz MPS46 Photoautomat, Linkam

(22) Possibly high-resolution analyses of well-aligned samples would show a difference.

(23) Reference 3b and refs 5d–e and 8 therein.

(24) (a) Tabushi, I.; Yamamura, K.; Okada, Y. *J. Org. Chem.* **1987**, *52*, 2502. (b) Tabushi, I.; Yamamura, K.; Okada, Y. *Tetrahedron Lett.* **1987**, *28*, 2269.

(25) Budig, H.; Lunkwitz, R.; Paschke, R.; Tschierske, C.; Nütz, U.; Diele, S.; Pelzl, G. *J. Mater. Chem.* **1996**, *6*, 1283.

(26) Collard, D. M.; Lillya, C. P. *J. Org. Chem.* **1991**, *56*, 6064.

(27) Clarkson, G. J.; McKeown, N. B.; Treacher, K. E. *J. Chem. Soc., Perkin Trans. 1* **1995**, 1817.

(28) The effects of benzene-containing side chains on the aggregation of triphenylenes can be seen in the data of (a) Destrade, C.; Mondon, M. C.; Malthete, J. *J. Phys. Colloq.* **1979**, *40*, 3 (see Table 2) and (b) Nguyen, H. T.; Gasparoux, H.; Destrade, C. *Mol. Cryst. Liq. Cryst.* **1981**, *68*, 101 (see Table 1).

(29) Leisen, J.; Werth, M.; Boeffel, C.; Spiess, H. W. *J. Chem. Phys.* **1992**, *97*, 3749.

LTS 350 hot stage, and Linkam TP 92 controller was used for optical characterization. The microscope, which has a dual beam splitter, was equipped with a video recording system comprising a Sony DXC-970MD CCD camera, JVC SRS-970 video recorder, Sony PVM-1353MD color monitor, and a computer with a Scion Image PR-CG7-PCI frame grabber card. A Perkin-Elmer DSC Pyris 7 with a Perkin-Elmer Pyris thermal analysis data station was used to analyze transition temperatures and heats of fusion. A Seiko Dual TG/DTA 320 instrument was used for thermogravimetric/differential thermal analyses. Two X-ray diffractometers were used. One was an Inel system with CPS 120 detector, XRG 2000 generator, Cu K α radiation, Minco CT 137 temperature controller (accurate to ± 1 °C), and a home-built heating stage. The other was a Siemens system (flat camera 2D-Xe-detector, 256×256 cells, Instec HS 400 hot stage and STC 200 controller, Rigaku RV-300 rotating anode, Ni-filtered Cu K α radiation). Mica, NBS silicon, and silver behenate were used as calibration standards. Lindemann capillaries (1.5 mm) were filled with ca. 15-mg samples.

Preparative Experiments. The required (+)-, (–)-, and (\pm)-tris(triisopropylsiloxy)[6]helicenes (**9**),⁸ +**H3C12**,⁸ +**H2C12**,⁷ chloromethoxydodecane,¹³ and 3-(dodecylthio)propanoic acid,¹⁴ were prepared by published procedures. 3,7-Dimethyl-1-iodooctanes¹⁰ were prepared from (S)-(-)- β -citronellol (Aldrich, 99%) and racemic β -citronellol (Aldrich, 95%) by hydrogenation over PtO₂, reaction with *p*-toluenesulfonyl chloride in pyridine, and heating to 80 °C with NaI in 3-pentanone.³⁰ Methyl 4-hydroxybenzoate (99%) and CsF (99%) were purchased from Acros, 1-iodododecane (98%) was obtained from Avocado, and BF₃·Et₂O (purified, redistilled) and Bu₄NF (1 M, in THF) were purchased from Aldrich. Purchased chemicals were used as received. Acetone was dried over 4 Å molecular sieves. DMF was passed under argon through two columns of 4 Å molecular sieves, and THF was similarly passed through alumina. The matrix for FAB mass spectrometry was *m*-nitrobenzyl alcohol.

Methyl 4-Dodecyloxybenzoate. Methyl 4-hydroxybenzoate (1.2 g, 7.9 mmol), K₂CO₃ (2.7 g, 20 mmol), and 1-iodododecane (2 mL, 8.1 mL) dissolved in acetone (15 mL, dried over 4 Å molecular sieves) were refluxed under N₂ for 8 h. The mixture was poured into water, extracted with EtOAc, washed with water and brine, dried over Na₂SO₄, and stripped of solvent. Chromatography (eluent, hexanes–EtOAc, 95:5–90:10) gave 1.72 g of product (a 68% yield). Mp 53–55 °C. IR (KBr) 2919, 2850, 1725, 1609, 1511, 1469, 1436, 1318, 1283, 1258, 1171, 1109, 1023 cm⁻¹. ¹H NMR (CDCl₃, 400 MHz) δ 7.97 (d, 8.9 Hz, 2H), 6.90 (d, 8.9 Hz, 2H), 4.00 (t, 6.6 Hz, 2H), 3.88 (s, 3H), 1.79 (m, 2H), 1.45 (m, 2H), 1.26 (bs, 16H), 0.88 ppm (t, 6.8 Hz, 3H). ¹³C NMR (CDCl₃, 75 MHz) δ 166.9, 162.9, 131.5, 122.3, 114.0, 68.2, 51.8, 31.9, 29.64, 29.58, 29.36, 29.1, 26.0, 22.7, 14.1 ppm. UV–vis ($c = 2.8 \times 10^{-5}$ M, dodecane) λ_{\max} (log ϵ) 253 nm (4.22). HRMS (FAB) m/z calcd for [M + H]⁺, C₂₀H₃₃O₃ 321.2430; found, 321.2404.

4-Dodecyloxyphenylmethanol. Dry THF (20 mL) was slowly added under N₂ to a mixture, cooled by an ice-bath, of methyl 4-dodecyloxybenzoate (1.72 g, 5.37 mmol) and LiAlH₄ (0.6 g, 16 mmol). After the mixture had stirred at room temperature for 2 h and then had been cooled with an ice bath, saturated aqueous NH₄Cl (20 mL) was added followed by 1 M HCl (50 mL). Extraction with ether (2 \times 50 mL), drying (MgSO₄), evaporation, and vacuum-drying gave 1.57 g (a 100% yield) of the pure alcohol. Mp 65–67 °C. IR (KBr) 3315, 3219, 2920, 2852, 1613, 1513, 1469, 1256, 1018 cm⁻¹. ¹H NMR (CDCl₃, 400 MHz) δ 7.28 (d, 8.6 Hz, 2H), 6.88 (d, 8.6 Hz, 2H), 4.61 (d, 5.5 Hz, 2H), 3.95 (t, 6.6 Hz, 2H), 1.78 (m, 2H), 1.51 (t, 5.7, –OH \sim 1H), 1.45 (m, 2H), 1.39–1.21 (m, 16H), 0.88 ppm (t, 6.8 Hz, 3H). ¹³C NMR (CDCl₃, 75 MHz) δ 158.8, 132.8, 128.6, 114.5, 68.0, 65.1, 31.9, 29.6, 29.4, 29.2, 26.0, 22.7, 14.1 ppm. UV–vis ($c = 7.9 \times 10^{-4}$ M, CH₃CN) λ_{\max} (log ϵ) 275 (3.16), 226 nm (4.03). HRMS (FAB) m/z calcd for C₁₉H₃₂O₂, 292.2402; found, 292.2389.

1-Dodecyloxy-4-iodomethylbenzene. BF₃·Et₂O (560 μ L, 4.42 mmol) was added in drops to a mixture, under N₂ and cooled in an ice-bath, of 4-dodecyloxyphenylmethanol (900 mg, 3.08 mmol) and KI (770 mg, 4.64 mmol) in dry dioxane (15 mL).¹² The reaction mixture was stirred for 90 min at room temperature, during which time the progress of the reaction was monitored by TLC, and then poured into water. Extraction with hexane (2 \times); washing with water, saturated aqueous NaHSO₃, and brine; drying over Na₂SO₄; and evaporation of the solvent gave 1.19 g of white product. Attempts to obtain an analytically pure sample by means of chromatography increased the amounts of impurities and decomposed the desired compound. IR (KBr) 2918, 2850, 1611, 1513, 1474, 1253, 1156, 1036, 825 cm⁻¹. ¹H NMR (CDCl₃, 400 MHz) δ 7.30 (d, 8.7 Hz, 2H), 6.81 (d, 8.7 Hz, 2H), 4.48 (s, 2H), 3.93 (t, 6.6 Hz, 2H), 1.76 (m, 2H), 1.44 (m, 2H), 1.40–1.20 (bs, 16H), 0.88 ppm (t, 6.8 Hz, 3H). ¹³C NMR (CDCl₃, 75 MHz) δ 158.8, 131.0, 114.8, 68.0, 31.9, 29.6, 29.4, 29.2, 26.0, 22.7, 14.1, 6.9 ppm. HRMS (FAB) m/z calcd for [M + H]⁺ C₁₉H₃₂IO, 403.1498; found, 403.1507.

(+)-(P)-Tris-(4-Dodecyloxybenzyloxy)[6]helicenebisquinone (+H3bn12). Dry DMF (1 mL) was added under N₂ to a mixture of (+)-(P)-tris(triisopropylsiloxy)[6]helicene [(+)-**9**], 41 mg, 45 μ mol, CsF (49 mg, 322 μ mol), and 1-dodecyloxy-4-iodomethylbenzene (201 mg, 0.5 mmol), and after the reaction mixture had stirred overnight at room temperature, it was poured into water. Extraction with toluene (2 \times), washing with water and brine, drying over Na₂SO₄, evaporation, chromatography on silica gel (eluent, toluene–EtOAc, 99:1), and preparative TLC (eluent, toluene–EtOAc 95:5) gave 28 mg (a 49% yield) of pure red wax. $[\alpha]_D + 653$ ($c = 1.92 \times 10^{-5}$ g/mL, dodecane). IR (film, NaCl window) 2924, 2854, 1660, 1612, 1513, 1302, 1246, 1226, 1175, 1086, 1010 cm⁻¹. ¹H NMR (CDCl₃, 400 MHz) δ 8.43 (s, 1H), 8.42 (s, 1H), 7.72 (s, 1H), 7.62 (s, 1H), 7.59 (s, 1H), 7.47 (2d, 8.7 Hz, 4H), 7.40 (d, 8.6 Hz, 2H), 6.99 (d, 8.5 Hz, 2H), 6.97 (d, 8.5 Hz, 2H), 6.91 (d, 8.6 Hz, 2H), 6.77 (d, 10.1 Hz, 1H), 6.75 (d, 10.1 Hz, 1H), 6.64 (d, 10.1 Hz, 1H), 6.59 (d, 10.1 Hz, 1H), 5.43 (d, 10.9 Hz, 1H), 5.40 (d, 10.9 Hz, 1H), 5.28 (m, 4H), 3.99 (m, 6H), 1.80 (m, 6H), 1.47 (m, 6H), 1.27 (bs, 48H), 0.88 ppm (m, 9H). ¹³C NMR (CDCl₃, 75 MHz): see the Supporting Information. UV–vis ($c = 1.53 \times 10^{-5}$ M, dodecane) λ_{\max} (log ϵ) 229 (4.52), 247 (4.49), 305 (4.44), 378 (3.73), 454 nm (3.70). CD ($c = 1.53 \times 10^{-5}$ M, dodecane) $\lambda(\Delta\epsilon)$ 432 (16), 359 (44), 299 (–35), 266 (16), 253 (15), 230 (–21), 218 nm (12). Anal. Calcd for C₈₃H₁₀₂O₁₀: C, 79.14; H, 8.16. Found: C, 78.83; H, 8.41.

(+)-(P)-Tris-(dodecyloxymethoxy)[6]helicenebisquinone (+H3C130). A mixture of (+)-(P)-tris(triisopropylsiloxy)[6]helicene [(+)-**9**], 43 mg, 47 μ mol and CsF (52 mg, 342 μ mol) in dry DMF (1.7 mL) was stirred under N₂ for 1 min, whereupon it turned green. Chloromethoxydodecane¹³ (344 mg, 1.47 mmol) was syringed in, and the reaction mixture was stirred at room temperature for 30 min. Saturated aqueous NaHCO₃ (5 mL) was added, and the mixture was extracted with EtOAc, washed with H₂O and brine, dried over Na₂SO₄, and freed of solvent. The product obtained by chromatography (eluent, toluene–EtOAc, 98:2), dissolved in the minimal amount of CH₂Cl₂, was precipitated by the addition of MeOH, filtered through a pad of Celite, washed with cold MeOH, and dissolved in CH₂Cl₂. Evaporation and vacuum-drying gave 37 mg (a 75% yield) of red waxy +**H3C130**. $[\alpha]_D + 1162$ ($c = 2.03 \times 10^{-5}$ g/mL, dodecane). IR (film, NaCl window) 2924, 2854, 1657, 1509, 1154, 1000, 935 cm⁻¹. ¹H NMR (CDCl₃, 400 MHz) δ 8.44 (s, 2H), 7.94 (s, 1H), 7.73 (s, 1H), 7.72 (s, 1H), 6.78 (d, 10.1 Hz, 1H), 6.76 (d, 10.1 Hz, 1H), 6.63 (d, 10.1 Hz, 1H), 6.59 (d, 10.1 Hz, 1H), 5.70–5.55 (m, 6H), 3.80 (m, 6H), 1.63 (m, 6H), 1.42–1.15 (m, 54H), 0.87 ppm (m, 9H). ¹³C NMR (CDCl₃, 75 MHz) δ 185.9, 185.7, 185.2, 157.1, 156.3, 153.6, 140.5, 140.2, 136.3, 136.2, 132.3, 131.4, 129.4, 128.6, 128.4, 128.1, 127.8, 127.6, 123.0, 122.2, 105.3, 104.9, 102.0, 94.5, 94.4, 70.5, 70.3, 70.0, 32.3, 30.0, 29.8, 26.5, 23.1, 14.6 ppm. UV–vis ($c = 1.97 \times 10^{-5}$ M, dodecane) λ_{\max} (log ϵ) 239 (4.74), 305 (4.55), 370 (3.91), 444 nm (3.78). CD ($c = 1.97 \times 10^{-5}$ M, dodecane) $\lambda(\Delta\epsilon)$ 219 (16), 227 (–9), 267 (10), 298 (–24), 357 (44), 441 nm

(30) The procedure was adapted from Jullien, L.; Canceill, J.; Lacombe, L.; Lehn, J.-M. *J. Chem. Soc., Perkin Trans. 2* **1994**, 989.

(15). Anal. Calcd for $C_{65}H_{92}O_{10}$: C, 75.54; H, 8.97. Found: C, 75.76; H, 8.67.

(±)-Tris-[3-(dodecylthio)propanoyloxy][6]helicenebis-quinone [±H3C14S]. 3-(Dodecylthio)propanoyl chloride (450 mg, 1.53 mmol), prepared by combining the corresponding acid¹⁴ with oxalyl chloride in benzene, was added to a mixture of racemic helicene (+)-**9** (64 mg, 71 μ mol), CsF (55 mg, 360 μ mol), and DMAP (12 mg, 100 μ mol) in DMF (1 mL). The reaction mixture was stirred at room temperature for 3 h and then poured into 1 M HCl. The material obtained by extraction with toluene (2 \times), washing with water and brine, drying over Na_2SO_4 , and evaporation was dissolved in the minimum amount of CH_2Cl_2 and precipitated by the addition of MeOH. Evaporation reduced the volume by ca. $1/3$, and the solid precipitate was isolated by filtering the mixture through Celite, washing with MeOH, and using CH_2Cl_2 to dissolve the product from the filter. Chromatography (eluent, toluene containing 2–3% EtOAc) gave 45 mg (a 53% yield) of orange product. IR (film, NaCl window) 2923, 2853, 1769, 1662, 1112 cm^{-1} . 1H NMR ($CDCl_3$, 400 MHz) δ 8.25 (d, 8.9 Hz, 1H), 8.21 (d, 8.9 Hz, 1H), 8.09 (s, 1H), 8.08 (s, 1H), 8.07 (s, 1H), 6.86 (d, 10.2 Hz, 1H), 6.85 (d, 10.2 Hz, 1H), 6.70 (d, 10.2 Hz, 1H), 6.68 (d, 10.2 Hz, 1H), 3.10 (m, 6H), 3.03 (m, 6H), 2.65 (m, 6H), 1.66 (m, 6H), 1.43 (m, 6H), 1.28 (bs, 48H), 0.87 (m, 9H). ^{13}C NMR ($CDCl_3$, 75 MHz) δ 185.0, 183.7, 169.8, 169.6, 169.4, 150.1, 149.8, 147.3, 139.8, 139.7, 136.3, 136.2, 132.7, 132.3, 131.3, 130.9, 129.4, 129.2, 128.9, 128.0, 127.6, 123.1, 122.4, 116.2, 113.3, 35.1, 32.3, 31.9, 29.6, 29.4, 29.3, 28.9, 27.0, 26.9, 22.7, 14.1 ppm. UV–vis ($c = 1.19 \times 10^{-5}$ M, hexane) λ_{max} (log ϵ) 241 (4.39), 293 (4.26), 355 (3.76), 411 nm (3.43). Anal. Calcd for $C_{71}H_{96}O_{10}S_3$: C, 70.73; H, 8.03. Found: C, 70.53; H, 8.26.

(+)-Tris-[3-(3,7-dimethyloctyloxy)-(P)-[6]helicenebis-quinone [±H3C10rac]. A 1 M solution of Bu_4NF (100 μ L) in THF was added in drops during 2 h to a mixture at 70 °C of (+)-(*P*)-tris(triisopropylsiloxy)[6]helicene (27.5 mg, 30 μ mol) and racemic 1-iodo-3,7-dimethyloctane (270 mg, 1 mmol), in THF (0.75 mL), and the reaction mixture was stirred at 70 °C for two more hours. It was then poured into water. Extraction with hexane, washing with water and brine, drying over Na_2SO_4 , evaporation, and chromatography (eluent, hexanes–EtOAc, 90:10–85:15) gave 11 mg (a 42% yield) of red waxy product. $[\alpha]_D + 1306$ ($c = 1.34 \times 10^{-5}$ g/mL, hexane). IR (film, NaCl window) 2954, 2927, 1657, 1509 cm^{-1} . 1H NMR ($CDCl_3$, 400 MHz) δ 8.43 (s, 2H), 7.63 (s, 1H), 7.49 (s, 1H), 7.48 (s, 1H), 6.76 (d, 10.0 Hz, 1H), 6.74 (d, 9.6 Hz, 1H), 6.62 (d, 10.1 Hz, 1H), 6.58 (d, 10.1 Hz, 1H), 4.48–4.30 (m, 6H), 2.06 (m, 3H), 1.83 (m, 6H), 1.60 (m, 3H), 1.50–1.15 (m, 18H), 1.05 (m, 9H), 0.90 ppm (m, 18H). ^{13}C NMR ($CDCl_3$, 100 MHz) δ 185.5, 185.1, 158.7, 157.5, 155.1, 140.2, 139.9, 135.8, 135.6, 133.7, 131.6, 131.0, 129.0, 128.0, 127.9, 127.5, 127.2, 126.6, 122.6, 121.7, 102.2, 101.8, 98.6, 67.8, 67.1, 39.3, 37.3, 36.1, 30.4, 30.3, 30.2, 30.0, 28.0, 24.9, 24.8, 24.7, 22.7, 22.6, 19.9, 19.8, 19.7 ppm. UV–vis ($c = 1.97 \times 10^{-5}$ M, dodecane) λ_{max} (log ϵ) 239 (4.74), 305 (4.55), 370 (3.91), 444 nm (3.78). CD ($c = 1.97 \times 10^{-5}$ M, dodecane) $\lambda(\Delta\epsilon)$ 219 (16), 227 (–9), 267 (10), 298 (–24), 357 (44), 441 nm (15). HRMS (FAB) m/z calcd for $C_{56}H_{72}O_7$, 856.5278; found, 856.5287.

(+)-(*P*)-Tris-[3-(3,7-dimethyloctyloxy)[6]helicenebis-quinone [±H3C10S]. Bu_4NF in THF (1 M, 100 μ L) was added to a solution of (+)-(*P*)-tris(triisopropylsiloxy)[6]helicene [(+)-**9**], 27.5 mg, 30 μ mol and (*S*)-1-iodo-3,7-dimethyloctane (270 mg, 1 mmol) in DMF (0.5 mL), which was then heated at 50 °C for 3 h. The mixture was poured into water, and after extraction with hexane, washing with water and brine, drying

(Na_2SO_4), evaporation, and chromatography (eluent, hexanes–EtOAc, 90:10–85:15), gave material that was dissolved in the minimum amount of CH_2Cl_2 and precipitated by the addition of MeOH (ca. 15 mL). After evaporation had reduced the volume by ca. $1/4$, the solid was filtered with Celite, washed with MeOH, and washed from the filter with CH_2Cl_2 . Obtained was 12 mg (46%) of red material. $[\alpha]_D + 1832$ ($c = 1.49 \times 10^{-5}$ g/mL, hexane). IR (film, NaCl window) 2953, 2925, 1658, 1509 cm^{-1} . 1H NMR ($CDCl_3$, 400 MHz) δ 8.43 (s, 2H), 7.63 (s, 1H), 7.49 (s, 1H), 7.48 (s, 1H), 6.76 (d, 10.0 Hz, 1H), 6.74 (d, 9.6 Hz, 1H), 6.62 (d, 10.1 Hz, 1H), 6.58 (d, 10.1 Hz, 1H), 4.48–4.30 (m, 6H), 2.06 (m, 3H), 1.83 (m, 6H), 1.60 (m, 3H), 1.50–1.15 (m, 18H), 1.05 (m, 9H), 0.90 ppm (m, 18H). ^{13}C NMR ($CDCl_3$, 75 MHz) δ 185.5, 185.2, 158.7, 157.5, 155.1, 140.2, 139.9, 135.8, 135.6, 133.6, 131.6, 130.9, 129.0, 128.0, 127.8, 127.5, 127.1, 126.6, 122.6, 121.7, 102.2, 101.8, 98.5, 67.8, 67.1, 39.2, 37.3, 36.0, 30.3, 30.1, 30.0, 29.7, 28.0, 24.9, 24.8, 22.7, 22.6, 19.9, 19.8, 19.7 ppm. UV–vis ($c = 1.74 \times 10^{-5}$ M, hexane) λ_{max} (log ϵ) 452 (3.67), 305 (4.41), 239 nm (4.57). CD ($c = 1.74 \times 10^{-5}$ M, hexane) $\lambda(\Delta\epsilon)$ 446 (16), 431 (16), 356 (44), 299 (–34), 267 (15), 228 (–25), 217 nm (15). HRMS (FAB) m/z calcd for $C_{56}H_{72}O_7$, 856.5278; found, 856.5240.

(–)-(*M*)-Tris-[3-(3,7-dimethyloctyloxy)[6]helicenebis-quinone [–H3C10S]. The same procedure applied to 33.5 mg of (–)-(*M*) tris(triisopropylsiloxy)[6]helicene [(–)-**9**], 350 mg of (*S*)-1-iodo-3,7-dimethyloctane, 0.75 mL of DMF, and 110 μ L of 1 M Bu_4NF in THF gave 15 mg (48%) of red waxy product. $[\alpha]_D - 701$ ($c = 1.77 \times 10^{-5}$ g/mL, hexane). IR (film, NaCl window) 2950, 2923, 1658, 1509 cm^{-1} . 1H NMR ($CDCl_3$, 400 MHz) δ 8.43 (s, 2H), 7.63 (s, 1H), 7.49 (s, 1H), 7.48 (s, 1H), 6.76 (d, 10.0 Hz, 1H), 6.74 (d, 9.6 Hz, 1H), 6.62 (d, 10.1 Hz, 1H), 6.58 (d, 10.1 Hz, 1H), 4.48–4.30 (m, 6H), 2.06 (m, 3H), 1.83 (m, 6H), 1.60 (m, 3H), 1.50–1.15 (m, 18H), 1.05 (m, 9H), 0.90 ppm (m, 18H). ^{13}C NMR ($CDCl_3$, 75 MHz) δ 185.5, 185.2, 158.7, 157.5, 155.1, 140.2, 139.8, 135.8, 135.6, 133.6, 131.6, 130.9, 129.0, 128.0, 127.8, 127.5, 127.1, 126.6, 122.6, 121.7, 102.2, 101.8, 98.5, 67.8, 67.1, 39.2, 37.3, 36.0, 30.3, 30.1, 29.7, 28.0, 24.9, 24.8, 22.7, 22.6, 19.9, 19.8, 19.7 ppm. UV–vis ($c = 2.06 \times 10^{-5}$ M, hexane) λ_{max} (log ϵ) 453 (3.59), 305 (4.26), 241 nm (4.37). CD ($c = 2.06 \times 10^{-5}$ M, hexane) $\lambda(\Delta\epsilon)$ 446 (–11), 429 (–12), 357 (–38), 298 (22), 268 (–15), 228 (16), 217 nm (–14). HRMS (FAB) m/z calcd for $C_{56}H_{72}O_7$, 856.5278; found, 856.5259.

Acknowledgment. We thank Professors Colin Nuckolls (Columbia University) and Timothy Swager (MIT) for advice and for the use of their equipment. This work was supported at Columbia University by the National Science Foundation, in part by NSF Award CHE0094723 and in part by the Foundation's Nanoscale Science and Engineering Initiative under NSF Award CHE0117752. L.V. thanks Alfred P. Bader for a Bader fellowship. The work at the University of Windsor was supported by NEDO and the National Sciences and Engineering Research Council of Canada.

Supporting Information Available: 1H and ^{13}C NMR, IR, UV, and CD spectra of the compounds prepared (PDF). This material is available free of charge via the Internet at <http://pubs.acs.org>.

CM034146J